The Astronomical Journal, 153:35 (13pp), 2017 January doi:10.3847/1538-3881/153/1/35

INFRARED SPECTROSCOPY OF SYMBIOTIC STARS. XI. ORBITS FOR SOUTHERN S-TYPE SYSTEMS: HEN 3-461, SY MUS, HEN 3-828, AND AR PAV

Francis C. Fekel[1], Kenneth H. Hinkle[2], Richard R. Joyce[2], and Peter R. Wood[3]
[1] Tennessee State University, Center of Excellence in Information Systems, 3500 John A. Merritt Boulevard, Box 9501, Nashville, TN 37209 USA; fekel@evans.tsuniv.edu
[2] National Optical Astronomy Observatory, P.O. Box 26732, Tucson, AZ 85726 USA; hinkle@noao.edu, joyce@noao.edu
[3] Research School of Astronomy and Astrophysics, Mount Stromlo Observatory, Australian National University, Cotter Road, Weston Creek, ACT 2611, Australia; wood@mso.anu.edu.au
Received 2016 October 5; revised 2016 November 21; accepted 2016 November 22; published 2016 December 29

ABSTRACT

Employing new infrared radial velocities, we have computed spectroscopic orbits of the cool giants in four southern S-type symbiotic systems. The orbits for two of the systems, Hen 3-461 and Hen 3-828, have been determined for the first time, while orbits of the other two, SY Mus and AR Pav, have previously been determined. For the latter two systems, we compare our results with those in the literature. The low mass of the secondary of SY Mus suggests that it has gone through a common envelope phase. Hen 3-461 has an orbital period of 2271 days, one of the longest currently known for S-type symbiotic systems. That period is very different from the orbital period proposed previously from its photometric variations. The other three binaries have periods between 600 and 700 day, values that are typical for S-type symbiotic orbits. Basic properties of the M giant components and the distance to each system are determined.

Key words: binaries: symbiotic – infrared: stars – stars: late-type

1. INTRODUCTION

Symbiotic stars are long-period, mass-transfer binaries that contain two evolved stars, typically an M giant primary and a compact companion. Although the giant's companion is usually a white dwarf, in at least one case it is a neutron star (Hinkle et al. 2006). From their characteristics at infrared wavelengths (Webster & Allen 1975) these systems have been divided into two subclasses, S for stellar-type and D for dusty-type systems. The S-type systems generally have periods in the 1–5 year range (Mikołajewska 2003). The D-type systems contain Mira variables (e.g., Whitelock 1987), and as a result of their huge radii, the orbital periods of those binaries are an order of magnitude or greater than those of S-type systems (Schmid & Schild 2002; Hinkle et al. 2013).

An important step in our understanding of such evolved binary systems is the determination of their orbital periods and other orbital elements. Belczyński et al. (2000) compiled a catalog of basic properties for nearly 200 symbiotic stars. More recently, Gromadzki et al. (2013) searched the large photometric surveys of ASAS, MACHO, and OGLE for symbiotic stars, analyzed their light curves, and estimated their orbital periods. As a result of that survey and previous work, more than 50% of the S-type systems listed in Belczyński et al. (2000) currently have their periods estimated (Mikołajewska 2012).

A complete determination of the orbital elements of the cool giant in symbiotic binaries is complicated by several factors. Nebular emission contaminates the spectrum of symbiotics at blue and even at times red wavelengths, so spectroscopic observations of the cool giant are best obtained in the infrared. About 50% of the symbiotics in the catalog of Belczyński et al. (2000) have $V \geqslant 13.0$ mag, so precise velocities from high-resolution spectra require at least a moderate aperture telescope. The long-period orbits have low velocity amplitudes, and the orbital analysis can be complicated by additional velocity variations caused by pulsation. These problems contribute to the difficulty in obtaining well-determined orbital elements. At present, about 40 of the cool giant components in S-type symbiotics have had their orbital elements computed (Mikołajewska 2011; Jorissen et al. 2012). This is about 20% of the systems in the catalog of Belczyński et al. (2000). Although the current number of known symbiotics is less than 300 (Miszalski et al. 2013), there have recently been spectroscopic searches for additional symbiotics, especially in the Galactic bulge, that have produced newly identified systems (Miszalski et al. 2013; Miszalski & Mikołajewska 2014).

In this paper we determine orbits for four southern S-type symbiotic systems, Hen 3-461, SY Mus, Hen 3-828, and AR Pav, and estimate the properties of the M giant components and the distance to each system. Two of the systems, SY Mus and AR Pav, have had previous orbit determinations. For those stars we compare our results with those in the literature. Some basic data for the four symbiotics are given in Table 1.

2. OBSERVATIONS AND REDUCTIONS

Our spectroscopic observations in the southern hemisphere were initially acquired from 2001 March through 2002 December. We observed at the Mount Stromlo Observatory (MSO), which is located near Canberra, Australia, and used the 1.88 m telescope and coudé spectrograph. The detector to record our spectra was an infrared camera, NICMASS, that was developed at the University of Massachusetts. It produced a 2 pixel resolving power of 44,000 at a wavelength of 1.623 μm. Joyce et al. (1998) and Fekel et al. (2000) have given a more extensive description of the setup.

The Canberra area bush fires of 2003 January destroyed both the 1.88 m telescope at MSO and our infrared NICMASS camera. This brought our observing program at that observatory to an unexpected and early end.

In an attempt to supplement the initial MSO observations, between 2003 February and 2010 June we obtained some additional spectra with the 8 m Gemini South telescope, located

Table 1
Basic Properties of the Program Stars

Name	V[a] (mag)	K[a] (mag)	$H-K$[a] (mag)	Cool Star Spectral Class[b]	Orbital Period (days)
Hen 3-461	12.26	3.84	0.37	M7	2271
SY Mus	10.67	4.70	0.30	M4.5	624.4
Hen 3-828	14.30	7.17	0.38	M6	660.5
AR Pav	11.14	7.10[c]	0.28[c]	M5	603.9

Notes.
[a] Munari et al. (1992) unless otherwise indicated.
[b] Mürset & Schmid (1999).
[c] Glass & Webster (1973).

at Cerro Pachon, Chile. We used the Phoenix cryogenic echelle spectrograph, which has been described extensively by Hinkle et al. (1998). That spectrograph enabled us to observe at several different infrared wavelength regions including 1.563, 2.226, and 2.364 μm, and the Gemini South spectra have a resolving power equal to either 50,000 or 70,000.

From 2009 May through 2010 June we also used the 1.5 m telescope at the Cerro Tololo Inter-American Observatory. That telescope is operated by the Small and Moderate Aperature Research Telescope System (SMARTS) consortium of universities and other organizations. During that time period, we acquired five spectra with the 1.5 m telescope, a fiber fed echelle spectrograph, and a 2K SITe CCD. The spectra have a resolving power of ~25,000 at 5500 Å.

Following Joyce (1992), we used standard observing and reduction techniques. Wavelength calibration and telluric line removal is discussed by Fekel et al. (2015).

The echelle spectrograms from the 1.5 m SMARTS telescope cover the wavelength range 4020–7300 Å. Unfortunately, the emission continuum from the gas around the secondary causes difficulty in detecting and measuring the late-type giant absorption line spectrum at blue and visual wavelengths. Thus, we chose to measure velocities in one of the reddest orders of the SMARTS echelle spectrograms at a wavelength region near 7130 Å.

In Figures 1 and 2 we plot representative spectra of the program stars at wavelengths of 1.563, and 2.226 μm, respectively. Those figures also include spectra of δ Oph, spectral type M0.5 III (Keenan & McNeil 1989), which we used as our primary velocity standard. At these wavelengths the vast majority of the lines come from the photosphere of the red giant. Fekel et al. (2010) have provided a more extensive discussion of the molecular and atomic lines that are found in the spectra of these two regions.

We measured radial velocities of the program stars with the IRAF cross-correlation program FXCOR (Fitzpatrick 1993). Our primary reference star was the M giant IAU radial velocity standard δ Oph, which was observed multiple times during the course of most nights. From time to time when spectra of δ Oph were not acquired, α Cet or several other M giants were used as velocity standards. The radial velocities of δ Oph and α Cet are -19.1 km s^{-1} and -25.3 km s^{-1}, respectively, from Scarfe et al. (1990). From our unpublished observations we adopted velocities of 21.3 km s^{-1} for HR 3718, 18.0 km s^{-1} for HR 4162, -32.2 km s^{-1} for HR 5150, 58.7 km s^{-1} for HR 5181, -9.6 km s^{-1} for HR 7900, and -22.8 km s^{-1} for HR 7951.

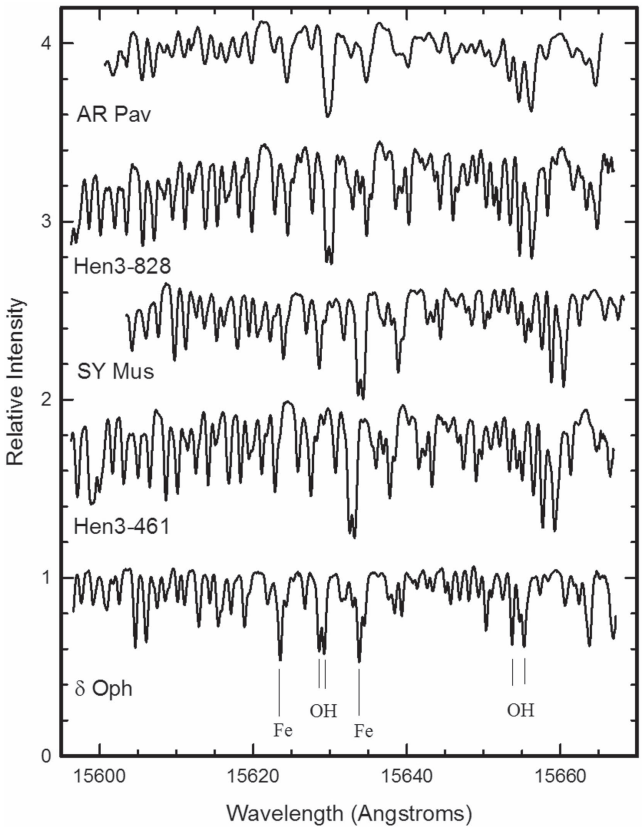

Figure 1. Spectra of Hen 3-461, SY Mus, Hen 3-828, AR Pav, and δ Oph at 1.563 μm observed with the Phoenix spectrograph on the Gemini South telescope. The relative intensity scales for Hen 3-461, SY Mus, Hen 3-828, and AR Pav have been offset by 0.9, 1.6, 2.4, and 3.1, respectively. No correction for telluric absorption lines is needed in this spectral region. Several lines have been identified.

3. ORBITAL ANALYSIS

For systems without known spectroscopic orbits, we used the computer program PGRAM (PeriodoGRAM), which compares the phased velocities for each trial period with a sine curve fit, to determine orbital periods. The sum of the squared velocity residuals from the fit was computed and the period having the smallest value of that sum was chosen as the best preliminary period. A sine curve fit works well to identify an approximate period even if the orbit has a moderate eccentricity.

With the best initial period for each system in hand, we then determined eccentric and circular orbital elements with several computer programs (Fekel et al. 2008). We note that for a circular orbit the element T, a time of periastron passage, is undefined. Therefore, following the recommendation of Batten et al. (1989), we used T_0, a time of maximum velocity, for our circular-orbit solutions.

4. PULSATION PERIOD SEARCH

All M giants have light variability from pulsation, and in general the later spectral type and higher luminosity stars have larger variability amplitudes (Percy et al. 2001). Semi-regular variables are defined as having amplitudes less than 2.5 mag. Their periods typically range from 30 to 200 days (Lebzelter & Hinkle 2002). Based on high-precision *Kepler* photometry, Hartig et al. (2014) discussed the stochastic behavior of the

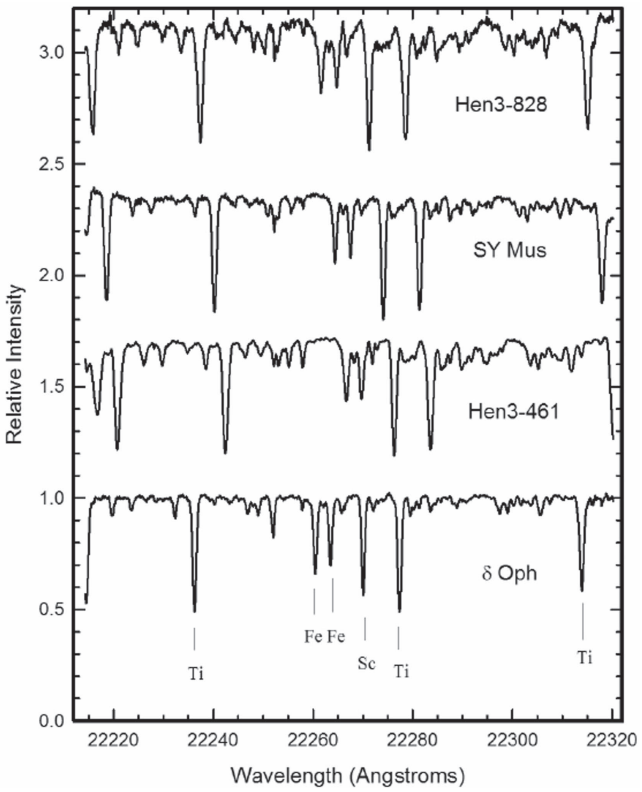

Figure 2. Spectra of Hen 3-461, SY Mus, Hen 3-828, and δ Oph at 2.226 μm observed with the Phoenix spectrograph on the Gemini South telescope. The relative intensity scales for Hen 3-461, SY Mus, and Hen 3-828 have been offset by 0.7, 1.4, and 2.1, respectively. The telluric spectrum has been ratioed out by referencing a hot star spectrum acquired on the same night. Several features are identified.

light curves of a number of semi-regular variables. In addition to the light variability, pulsation also causes velocity variations in semi-regular variables, which usually show amplitudes of up to a few km s^{-1} (e.g., Lebzelter & Hinkle 2002). Thus, part of the velocity variations seen in our symbiotic binaries likely comes from pulsation.

Having determined the orbital elements for our evolved giants, we searched for periodicities in the velocity residuals of our data and, when appropriate, the data in the literature with the program PGRAM. However, such an analysis brings with it a strong word of caution because both the number and distribution of the velocity observations are not well suited for the identification of the shorter pulsation periods. For example, our velocities range in number from 16 to 30, and our observations were generally acquired just two or sometimes three times per year over a 10 year period. Another factor is the low amplitudes, only about 1–2 km s^{-1}, of our best possible pulsation periods. With such a small number of observations, the phase placement of just a few velocities with large residuals can significantly change the results.

For three of the four stars, our velocity residuals are large enough to attempt an analysis. However, for AR Pav, which has only 16 velocities and an rms residual to the orbital fit of 0.5 km s^{-1}, we have not attempted to analyze our residuals, although we did examine the residuals for that star from other sources. We comment on our results in the individual star sections.

5. HEN 3-461 = IRAS 10370-5108 = PK 283+06 2

5.1. Short History

From an objective prism survey to find southern emission line stars Henize (1976) noted that the continuum of Hen 3-461 was very red and a TiO band was suspected, while the Hα emission feature was sharp and strong. Thus, he classified it as a probable symbiotic star. In his catalog of symbiotic stars Allen (1984) remained cautious and only listed it as a possible member. However, Pereira et al. (1998) acquired spectra of seven suspected symbiotics and found Hen 3-461 to have a strong late-type continuum with TiO absorption bands, Balmer emission features, and several weak forbidden emission lines. Thus, they concluded that Hen 3-461 is indeed a symbiotic star. Mürset & Schmid (1999) included the star in an infrared spectrum survey of over 90 symbiotics and classified its spectral class as M7. Luna et al. (2013) examined 41 symbiotic binaries and detected X-rays, which are evidence of mass transfer, for the first time in nine of the systems including Hen 3-461.

Munari et al. (1992) acquired optical and infrared photometry of 93 symbiotic binaries including Hen 3-461 (Table 1). Gromadzki et al. (2013) examined the ASAS database (Pojmanski 2002) light curve for Hen 3-461 and found a period of 635 days that they associated with the orbital period. They also examined the light curve residuals and detected a period of 79 days, which they ascribed to pulsation.

Gałan et al. (2016) analyzed high-dispersion infrared spectra of 24 S-type symbiotics to determine their abundances. They found that Hen 3-461 has a near solar iron abundance of [Fe/H] = 0.12 ± 0.11.

5.2. Spectroscopic Orbit

Between 2001 March and 2010 May we acquired 30 observations of Hen 3-461 at three observatories (Table 2). Our period search produced no evidence of the 635 day photometric period that was presumed by Gromadzki et al. (2013) to be the orbital period. In fact, our first 17 observations, which cover almost 600 days, show a nearly constant velocity of 31.9 ± 0.5 km s^{-1}. Instead, our initial analysis of the velocities produced a much longer period of 2116 days. Determination of the orbital elements resulted in a period of 2271 ± 17 days or 6.22 ± 0.05 years and a significant eccentricity of 0.40 ± 0.04. The full set of orbital elements is given in Table 3. Figure 3 compares our measured radial velocities and the computed radial velocity curve. Zero phase is a time of periastron.

5.3. Pulsation Period Search

The orbital periods of symbiotic stars can be determined from several types of light variability such as eclipses, reflection effect, and ellipsoidal variations (e.g., Mikołajewska 2001; Gromadzki et al. 2013). To identify such orbital periods, Gromadzki et al. (2013) examined the light curves of 79 symbiotic stars that had been observed in large photometric surveys. From ASAS data for Hen 3-461 they found a period of 635 days, which they identified as the orbital period. They also detected a shorter period of 79 days, which they ascribed to pulsation. Unlike many of their light curves, the one they presented for their identified orbital period of Hen 3-461 appears to be dominated by the short period variations. As mentioned in the previous section, we did not find a period of

Table 2
Radial Velocities of Hen 3-461

HJD −2400000	Phase	Velocity (km s^{-1})	$O-C$ (km s^{-1})	Observatory[a]
51988.096	0.698	31.6	−1.1	MSO
52043.960	0.723	32.8	0.5	MSO
52092.919	0.745	30.8	−1.1	MSO
52133.887	0.763	31.2	−0.4	MSO
52200.256	0.792	32.9	1.8	MSO
52253.220	0.815	31.7	0.8	MSO
52315.094	0.842	31.8	1.1	MSO
52349.089	0.857	32.0	1.3	MSO
52350.994	0.858	30.6	−0.1	MSO
52354.116	0.860	30.4	−0.3	MSO
52355.994	0.860	30.7	0.0	MSO
52358.161	0.861	30.8	0.1	MSO
52398.016	0.879	28.5	−2.4	MSO
52402.939	0.881	30.0	−0.9	MSO
52446.826	0.900	31.4	0.0	MSO
52451.881	0.903	31.2	−0.3	MSO
52452.812	0.903	32.6	1.1	MSO
52575.219	0.957	33.9	−1.1	MSO
52629.216	0.981	38.5	0.8	MSO
52686.777	0.006	41.0	0.2	Gem S
52749.566	0.034	43.3	−0.4	Gem S
52986.783	0.138	45.5	−0.4	Gem S
53098.608	0.187	43.5	−1.3	Gem S
53714.838	0.459	39.0	1.1	Gem S
53828.560	0.509	35.5	−1.2	Gem S
54923.558	0.991	39.9	0.9	Gem S
54969.510	0.011	41.9	0.4	CTIO
54975.480	0.014	40.7	−1.1	CTIO
55268.523	0.143	46.0	0.1	Gem S
55340.492	0.175	47.0	1.9	Gem S

Note.
[a] MSO—Mount Stromlo Observatory, Gem S—Gemini South Observatory, CTIO—Cerro Tololo Inter-American Observatory.

Table 3
Orbital Elements and Related Parameters of Hen 3-461

Parameter	Value
P (days)	2271 ± 18
T (HJD)	2452673 ± 31
γ (km s^{-1})	37.86 ± 0.31
K (km s^{-1})	7.81 ± 0.35
e	0.404 ± 0.045
ω (degree)	281.7 ± 8.3
$a \sin i$ (10^6 km)	223 ± 11
$f(m)$ ($M_\odot$)	0.086 ± 0.013
Standard error of an observation of unit weight (km s^{-1})	1.1

635 days in the radial velocities but rather a period of 2271 days. Examining the velocity residuals from our 2271 day orbit, we also did not find any evidence for the 79 ± 1 day period seen in the photometry. Instead, possible periods of 34.8 and 104.5 days were found. However, the phase plots of those periods did not lend strong support to the reality of those possible periodic variations.

5.4. Discussion

Munari et al. (1992) included Hen 3-461 in their optical and infrared photometric survey of symbiotic stars. As a result, they

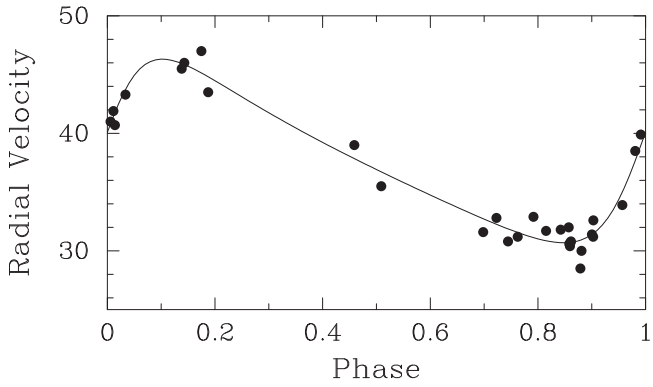

Figure 3. The M giant radial velocities of Hen 3-461 (filled circles) compared with its computed eccentric orbit (solid line). Zero phase is a time of periastron passage.

acquired $UBVR_cI_cJHK$ observations. Their values for V, K, and $J-K$ are 12.26, 3.84, and 1.50 mag, respectively. From an extensive spectrum analysis of TiO bands in the near-infrared Mürset & Schmid (1999) assigned its cool giant a spectral class of M7 making Hen 3-461 one of the coolest known symbiotics. Other symbiotics classified by Mürset & Schmid (1999) as M7 include CH Cyg, the longest period (15.6 years) S-type system known (Hinkle et al. 2009), and two D-type symbiotics, V1016 Cyg and HM Sge, which contain Mira variables and have estimated orbital periods of decades (Hinkle et al. 2013).

With a period of 6.2 years, Hen 3-461 has one of the longest periods known for an S-type system. For example, in an analysis of the light curves from large photometric surveys Gromadzki et al. (2013) concluded that 58 symbiotic systems showed light variability that they associated with the orbital period. Of those systems they found that only two, SS 73-122 and Hen 3-1591, have longer periods than Hen 3-461. However, unlike the vast majority of systems for which they identified orbital periods, they presented no light curve phased with their orbital period to support their claim for either of those two long-period systems. While the vast majority of photometric periods identified by Gromadzki et al. (2013) are likely to be orbital periods, our spectroscopic results for Hen 3-461 demonstrate that, at least in one instance, the true orbital period is very different from the supposed photometric orbital period. Thus, the determination of spectroscopic orbits will be valuable in confirming the photometric results for other symbiotic systems.

Citing the theoretical work of Zahn (1977), Schmutz et al. (1994) and Mürset et al. (2000) have argued that the giant star in most S-type symbiotics should be synchronously rotating. With that assumption in hand, they then estimated the radius of the late-type giant in several symbiotic binaries.

While this is a useful approach, the orbit of Hen 3-461 is not circular, but instead has a significant eccentricity of 0.40. For eccentric orbits Hut (1981) stated that the rotational angular velocity will tend to synchronize with that of the orbital motion at periastron. He called this situation pseudosynchronous rotation. For Hen 3-461 we calculated a pseudosynchronous period of 1056 days.

Assuming that the cool giant has pseudosynchronous rotation, its minimum radius can be determined from its projected rotational velocity and pseudosynchronous period. For Hen 3-461 Gałan et al. (2016) has determined a $v \sin i$

value of 7.4 ± 0.6 km s^{-1}. The resulting minimum radius (i.e., sin i = 1) is 154 ± 13 $R_\odot$.

The orbital elements for the M giant of Hen 3-461 produce a value called the mass function of the orbit. This value depends on three quantities, the primary and secondary masses and the orbital inclination (Batten et al. 1989). From Table 3 the mass function value for Hen 3-461 is rather large, 0.086 $M_\odot$. Mikołajewska (2003) summarized mass estimates for 16 symbiotic systems. She found that the cool giant masses range from 3.0 to 0.7 $M_\odot$ with a peak at about 1.6 $M_\odot$, while the compact hot companion masses are predominately between 0.4 and 0.9 $M_\odot$ with an average of 0.5 $M_\odot$. The center-of-mass velocity of Hen 3-461 is moderately large, 37.9 km s^{-1}, suggesting that it is not a particularly young system, and so its M giant mass is unlikely to be toward the higher end of the range.

If we adopt a typical mass of 1.5 $M_\odot$ for the M giant, then the minimum mass (sin i = 1) of the presumed compact secondary is 0.76 $M_\odot$. However, no evidence of eclipses was found by Gromadzki et al. (2013) for this system. Thus, if the inclination is reduced from 90° to 60°, then the mass of the secondary rises to 0.88 $M_\odot$. From the relation between the initial and final mass for DA white dwarfs, the progenitor of the 0.88 $M_\odot$ would have been a 4.5 $M_\odot$ main sequence star (Kalirai et al. 2008). In addition to its apparent lack of eclipses, an inclination of 60° has been chosen for Hen 3-461 because if the orientation of the orbits in the sky is random, then those with inclinations greater than or equal to 60° are as likely to be detected as those with inclinations less than or equal to 60° (Motz & Duveen 1977, p. 478). Increasing the adopted primary mass increases the mass of the secondary as well. However, going in the opposite direction and decreasing the adopted mass of the primary to 1.0 $M_\odot$ still results in a minimum secondary mass of 0.61 $M_\odot$, which increases to 0.70 $M_\odot$ if the inclination is reduced to 60°. Thus, it appears that the presumed compact secondary component of Hen 3-461 is more massive than that of the typical S-type symbiotic binary.

We adopt 1.5 $M_\odot$ for the primary, an orbital inclination of 60°, and the resulting secondary mass of 0.88 $M_\odot$. Those masses produce a secondary to primary mass ratio of 0.59. With the adopted inclination and the assumption that the orbital and rotational axes are parallel, so that the orbital and rotational inclinations are equal, the minimum radius of the M giant is increased from 154 to 178 ± 15 $R_\odot$.

An estimate of the cool giant radius can also be made from the results of Gałan et al. (2016). They assigned Hen 3-461 an effective temperature of 3200 K and adopted a gravity of log g = 0.0. Their values are based on the color–temperature–gravity calibrations discussed by Kučinskas et al. (2005) and Dumm & Schild (1998) and produce a radius of 203 ± 50 $R_\odot$. In addition, Dyck et al. (1998) determined angular diameters of late type giants. From their Figure 5 a linear radius of about 175 $R_\odot$ is indicated for a giant with the effective temperature of Hen 3-461. Thus, we adopt the value of 178 $R_\odot$ derived from its rotational velocity.

The separation of the components and their mass ratio determine the giant's effective Roche lobe radius (Eggleton 1983). Assuming masses of 1.5 and 0.88 $M_\odot$ for the giant and its hot companion, respectively, we determined the orbital semimajor axis from Kepler's third law. But because the orbit of Hen 3-461 is not circular, the separation of the stars varies, and so, we used the smaller periastron separation rather than the semimajor axis. With Equation (2) of Eggleton (1983), we determined an M giant Roche-lobe radius of 248 $R_\odot$. Our estimated radius of 178 $R_\odot$ would fill 72% of that minimum Roche lobe. Such a result is in agreement with the conclusion of Mürset & Schmid (1999), who found that symbiotics are almost always detached binaries. While our estimated radius does not fill its minimum Roche lobe, the lobe filling ratio is rather large. However, the Roche lobe size will increase, reducing the ratio, as the stars move from periastron to apastron. It would be of interest to obtain light curves near periastron at red or near-infrared wavelengths (e.g., Rutkowski et al. 2007) to see whether Hen 3-461 has ellipsoidal light variations.

Table 4
Assumed and Derived Properties of Hen 3-461

Parameter	Value	Reference
Cool giant:		
M ($M_\odot$)	1.5 (Adopted)	This work
v sin i (km s^{-1})	7.4 ± 0.6	Gałan et al. (2016)
R ($R_\odot$)	178 ± 15	This work
$T_{\rm eff}$ (K)	3200 ± 100	Gałan et al. (2016)
L ($L_\odot$)	2977 ± 625	This work
$M_{\rm bol}$ (mag)	−3.95 ± 0.23	This work
M_K (mag)	−7.14 ± 0.23	This work
Hot component:		
M ($M_\odot$)	0.88	This work
System:		
i (degree)	60 (Adopted)	This work
Distance (kpc)	1.6 ± 0.2	This work

For the M giant we adopted an effective temperature of 3200 ± 100 K from Gałan et al. (2016). That value and our estimated radius of 178 ± 15 $R_\odot$ result in a luminosity of 2977 ± 625 $L_\odot$, which corresponds to $M_{\rm bol}$ = −3.95 ± 0.23 mag. To estimate the distance to Hen 3-461, we used its K mag and $J-K$ color from Munari et al. (1992). We then determined a bolometric correction at K using the analytic expression of Bessell & Wood (1984). Those results produced M_K = −7.14 ± 0.23 mag, which resulted in a distance of 1.6 ± 0.2 kpc with no correction for reddening. Hen 3-461 lies about 77° from the Galactic center but only 6°.3 above the Galactic plane. Any reddening will be much less in the infrared compared to the visual (e.g., Schlegel et al. 1998). Including an extinction, A_K, value of 0.5 mag decreases the distance to 1.2 kpc. The various derived quantities are summarized in Table 4.

6. SY MUS = HD 100336 = HEN 3-667 = SS 73-32 = HV 3376

6.1. Short History

Cannon (Cannon & Pickering 1914) found the star SY Mus to have hydrogen emission lines and light variability of less than 1 mag. Uitterdijk (1934) measured its brightness on photographic plates acquired between 1910 and 1932 and found a well defined period of 625 days. The variability was confirmed by Greenstein (1937), who determined a similar period of 623.1 days from Harvard Observatory plates. Seen as an emission-lined star on objective prism plates of the

Michigan–Mount Wilson Hα survey of the southern hemisphere, Henize (1952) obtained a slit spectrum that showed emission lines of hydrogen, helium, nitrogen, and oxygen as well as an M-type absorption spectrum. In their survey of emission line objects in the southern Milky Way, Sanduleak & Stephenson (1973) found its emission spectrum to be similar to that of Z And, and also detected an absorption spectrum that they classified as M2. In his survey catalog of southern emission line stars Henize (1976) noted previous spectra that indicated that the star is a symbiotic. Allen (1984) listed it in his catalog of symbiotic stars and provided a low-resolution spectrum of the blue and visual regions that exhibited various emission features and an M giant continuum.

Michalitsianos et al. (1982) obtained two ultraviolet spectra of SY Mus that showed very different levels of its hot continuum and emission line strengths. One of the two explanations that they suggested was that this variability was caused by eclipses of the hot component. Kenyon & Bateson (1984) analyzed 30 years of visual observations, determined a 627 day periodicity similar to that found in previous analyses, and argued that the visual variability resulted from the reflection effect and an eclipse of the hot component. To confirm the eclipse hypothesis, Kenyon et al. (1985) obtained ultraviolet spectra at a time of light minimum and compared them with previously acquired spectra at other light variability phases. The strength of the strong ultraviolet emission lines decreased dramatically during light minimum, and so they concluded that the hot component of SY Mus is indeed eclipsed. The light variability period was reexamined by Pereira et al. (1995), who analyzed visual observations between 1954 and 1993, covering 22 cycles, and determined a period of 624.5 days. Nearly one decade later, Schmutz et al. (1994) adopted that photometric period and determined a spectroscopic orbit for the M giant component. Dumm et al. (1999) acquired additional spectra, reexamined the photometric period, and produced an improved spectroscopic orbit. Shortly thereafter, Harries & Howarth (2000) computed a spectropolarimetric orbit for the system. Rutkowski et al. (2007) analyzed near-infrared light curves of SY Mus that showed ellipsoidal light variations. Mürset & Schmid (1999) detemined a spectral class of M4.5 in agreement with the result of Schmutz et al. (1994). Gałan et al. (2016) found the iron abundance of the M giant to be slightly subsolar, [Fe/H] $= -0.15 \pm 0.08$.

6.2. Spectroscopic Orbit

Over the years period determinations of the light variability of SY Mus have all been close to 625 days (see Kenyon & Bateson 1984; Pereira et al. 1995). In addition, Schmutz et al. (1994) determined a period of 628 days from their radial velocities. Dumm et al. (1999) made a new analysis of the visual light curve that covered 26 orbits from which they derived a period of 624.9 ± 0.3 days. Thus, they adopted a period of 625 days for their new orbital solution, which combined their velocities with the earlier velocities of Schmutz et al. (1994). Dumm et al. (1999) also concluded that their eccentric solution was not significantly better than their circular orbit. This result and the fact that theory predicts a circular orbit led them to adopt the $e = 0$ solution.

Our 19 spectra were acquired between 2001 March and 2010 April and so cover 9 years or 5.3 cycles. Using our velocities, we first obtained an orbital solution with all the orbital elements allowed to vary. That solution produced a period of 628 ± 3 day and $e = 0.14 \pm 0.04$. For the final solution of our velocities we have chosen to follow Dumm et al. (1999) and adopt a period of 625 days and a circular orbit. We then computed a circular orbit solution of all 58 radial velocities, which cover nearly 22 years, and allowed the period to be a free parameter. The velocities from Schmutz et al. (1994) and Dumm et al. (1999) were shifted in zero point by $+0.8\,\mathrm{km\,s^{-1}}$. After comparing the variance of the orbital solution of Dumm et al. (1999) with that of our final circular orbital solution mentioned above, we assigned unit weights to the velocities of Schmutz et al. (1994) and Dumm et al. (1999), while our velocities were given weights of 0.2. The period for the combined data solution is $624.4 \pm 0.8\,\mathrm{km\,s^{-1}}$. Table 5 provides all the radial velocity observations used in the combined solution. Table 6 lists three sets of orbital elements, the solution of Dumm et al. (1999), the circular orbit solution of our data alone, and the combined data solution.

Radial velocities from the combined solution are compared with the computed circular orbit in Figure 4. Phase zero is a time of maximum velocity.

6.3. Pulsation Period Search

As part of a large survey of symbiotic stars, Gromadzki et al. (2013) examined the V band ASAS photometric data of SY Mus. After identifying the orbital period of 624.5 days in that data, they subtracted the orbital variation and found a period of 56 ± 1 days in the light residuals. For the M giant we adopt an effective temperature of 3400 ± 100 K from Gałan et al. (2016). The gravity of $\log g = 0.5$ used by Gałan et al. (2016) and a mass of $1.5\,M_{\odot}$ result in a radius of $114 \pm 27\,R_{\odot}$. That radius and an effective temperature of 3400 ± 100 K produce a luminosity of $1556 \pm 760\,L_{\odot}$ corresponding to $M_{\mathrm{bol}} = -3.25 \pm 0.52$ mag. From the photometry of Munari et al. (1992) the values for V, K, and $J-K$ are 10.67, 4.70, and 1.41 mag, respectively. With those K and $J-K$ values we used the relation of Bessell & Wood (1984) to compute a bolometric correction and determine $M_K = -6.37 \pm 0.52$ mag. From relations between pulsation period and K magnitude and observational results from the LMC (Soszyński et al. 2013), periods in the range ~30–80 days can be expected in M giants with this luminosity resulting from overtone pulsation. The ASAS photometric period is not found in our velocity residuals. Our best period in that range is 49.2 days. But a plot of the velocity residuals phased with that period does not produce convincing evidence that it is real. The orbital fit of Dumm et al. (1999) results in a small rms residual of $0.6\,\mathrm{km\,s^{-1}}$, so we did not search those velocity residuals.

6.4. Discussion

With a period of 624.4 days the circular orbit of SY Mus is typical of symbiotic systems analyzed to date. The distribution of symbiotic binary periods peaks around 600 days and the orbits are generally circular at such periods (Mikołajewska 2012).

For the late-type giant the $v \sin i$ values of Schmutz et al. (1994) and Gałan et al. (2016) are nearly identical, 7 ± 1 and $6.6 \pm 0.6\,\mathrm{km\,s^{-1}}$, respectively. Thus, from Schmutz et al. (1994) the minimum value of the giant radius determined from synchronous rotation is $86 \pm 13\,R_{\odot}$.

As noted earlier, SY Mus is an eclipsing system. Schmutz et al. (1994) estimate that the orbital inclination is greater than

Table 5
Radial Velocities of SY Mus

HJD −2400000	Phase	Velocity (km s^{-1})	$O-C$ (km s^{-1})	Weight	Observatory[a]
47356.500	0.235	13.9	−0.6	1.0	LSO
48405.500	0.915	20.6	0.2	1.0	LSO
48624.800	0.266	12.6	−0.3	1.0	LSO
48624.800	0.266	13.5	0.6	1.0	LSO
48624.800	0.266	13.5	0.6	1.0	LSO
48698.600	0.384	8.3	0.4	1.0	LSO
48699.600	0.386	7.5	−0.4	1.0	LSO
48757.600	0.479	6.2	0.2	1.0	LSO
48758.600	0.480	6.4	0.4	1.0	LSO
48759.600	0.482	6.0	0.0	1.0	LSO
48831.500	0.597	8.1	0.8	1.0	LSO
48832.500	0.599	7.8	0.4	1.0	LSO
49003.800	0.873	19.4	0.3	1.0	LSO
49003.800	0.873	18.7	−0.4	1.0	LSO
49038.700	0.929	19.6	−1.1	1.0	LSO
49039.700	0.931	20.4	−0.3	1.0	LSO
49040.700	0.932	20.8	0.0	1.0	LSO
49132.600	0.079	19.8	−0.7	1.0	LSO
49368.000	0.456	6.9	0.7	1.0	LSO
49725.000	0.028	21.3	0.0	1.0	LSO
49811.000	0.166	17.8	0.2	1.0	LSO
50149.000	0.707	10.7	−0.9	1.0	LSO
50173.000	0.746	13.8	0.3	1.0	LSO
50188.000	0.770	14.3	−0.4	1.0	LSO
50202.000	0.792	15.2	−0.5	1.0	LSO
50210.000	0.805	15.8	−0.5	1.0	LSO
50221.000	0.823	17.5	0.4	1.0	LSO
50237.000	0.848	19.4	1.2	1.0	LSO
50267.000	0.896	18.9	−1.0	1.0	LSO
50287.000	0.928	21.8	1.1	1.0	LSO
50304.000	0.956	22.2	1.0	1.0	LSO
50483.000	0.242	14.4	0.3	1.0	LSO
50500.000	0.269	12.7	−0.1	1.0	LSO
50515.000	0.293	11.3	−0.3	1.0	LSO
50531.000	0.319	9.7	−0.7	1.0	LSO
50559.000	0.364	8.0	−0.6	1.0	LSO
50591.000	0.415	7.2	0.2	1.0	LSO
50650.000	0.510	5.9	−0.1	1.0	LSO
50825.000	0.790	15.6	0.0	1.0	LSO
51990.017	0.656	8.0	−1.4	0.2	MSO
52044.005	0.742	11.7	−1.6	0.2	MSO
52094.016	0.822	16.4	−0.7	0.2	MSO
52131.922	0.883	21.3	1.8	0.2	MSO
52200.279	0.993	21.5	0.0	0.2	MSO
52315.123	0.177	17.4	0.2	0.2	MSO
52349.139	0.231	14.4	−0.2	0.2	MSO
52351.014	0.234	13.1	−1.4	0.2	MSO
52398.090	0.309	8.9	−2.0	0.2	MSO
52444.877	0.384	7.7	−0.2	0.2	MSO
52506.900	0.484	6.2	0.2	0.2	MSO
52575.248	0.593	7.0	−0.2	0.2	MSO
52687.757	0.773	14.4	−0.4	0.2	Gem S
52749.582	0.872	21.3	2.2	0.2	Gem S
52986.825	0.252	13.3	−0.3	0.2	Gem S
53828.577	0.601	5.7	−1.7	0.2	Gem S
54923.592	0.354	11.2	2.2	0.2	Gem S
55278.591	0.923	22.0	1.4	0.2	Gem S
55312.601	0.977	23.1	1.7	0.2	Gem S

Note.
[a] LSO—La Silla Observatory, MSO—Mount Stromlo Observatory, Gem S—Gemini South Observatory.

Table 6
Orbital Elements and Related Parameters of SY Mus

Parameter	Dumm et al. (1999)	Our Solution	Combined Solution
P (days)	625.0	625.0 (adopted)	624.36 ± 0.80
T_0 (HJD)	2450176[a]	2453455.2 ± 4.4	2451580.5 ± 2.6
γ (km s^{-1})	12.9	13.66 ± 0.29	13.706 ± 0.092
K (km s^{-1})	7.8	8.72 ± 0.45	7.76 ± 0.14
e	0.0 (adopted)	0.0 (adopted)	0.0 (adopted)
$a \sin i$ (10^6 km)	...	74.9 ± 3.9	66.6 ± 1.2
$f(m)$ ($M_\odot$)	...	0.0429 ± 0.0067	0.0302 ± 0.0017
Standard error of an observation of unit weight (km s^{-1})	...	1.3	0.6

Note.
[a] Time of hot component eclipse.

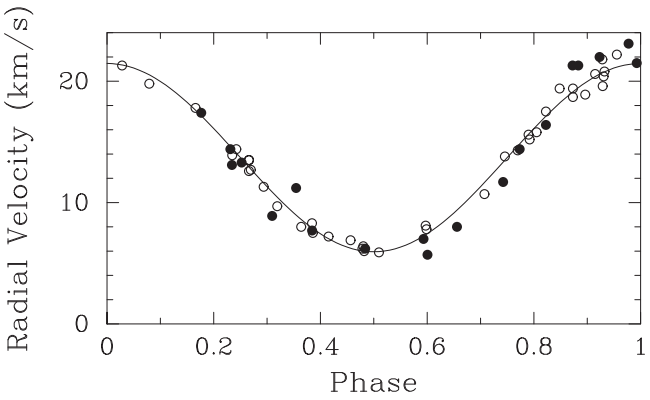

Figure 4. The M giant radial velocities of SY Mus are compared with its computed circular orbit (solid line). Filled circles represent our velocities, open circles represent those of Schmutz et al. (1994) and Dumm et al. (1999). Zero phase is a time of maximum velocity.

75°. From a spectropolarimetric orbital solution Harries & Howarth (2000) determined an inclination of 101° for the binary. From their analysis of infrared ellipsoidal light variations Rutkowski et al. (2007) obtained an inclination of 89°. From the latter two results we assume an inclination of 84°.

Adopting a typical mass of 1.5 $M_\odot$ for the cool giant and an inclination of 84°, the mass function value of the combined solution (Table 6) produces a mass of 0.50 $M_\odot$ for the secondary. Stellar evolutionary theory provides an additional check on the primary and secondary masses. Assuming that the stars evolve without significant mass exchange, the main sequence mass of the current degenerate secondary must have been larger than that of the current giant primary. From the white dwarf initial to final mass relation (Kalirai et al. 2008) a 0.50 $M_\odot$ white dwarf evolved from a 0.97 $M_\odot$ main sequence star. This initial mass is less massive than the adopted cool giant mass. The cool giant mass would need to be increased to 2.5 $M_\odot$, resulting in a 0.68 $M_\odot$ white dwarf secondary that evolved from a 2.6 $M_\odot$ main sequence star.

Rather than increasing the adopted mass of the cool giant, an alternative solution to the above problem for the SY Mus system is to assume that the white dwarf does indeed have a

low mass. In recent years many low mass white dwarfs have been discovered in binaries and likely result from common envelope evolution (Istrate et al. 2016).

Although we have adopted a mass of 1.5 $M_\odot$ for the cool giant, that mass may actually be too large. Both the 1.5 $M_\odot$ and the 2.5 $M_\odot$ primary mass values examined above have relatively rapid evolution with the age of a 1.5 $M_\odot$ star at the evolutionary stage of SY Mus being $\sim 3 \times 10^9$ years (e.g., Girardi et al. 2000). However, the slightly subsolar iron abundance found by Gałan et al. (2016) suggests that SY Mus may be even older, and thus, the primary mass may be less than 1.5 $M_\odot$. For a 1.0 $M_\odot$ primary the mass function and inclinaton demand a white dwarf mass of $\sim$0.4 $M_\odot$. Thus, although we have adopted a mass of 1.5 $M_\odot$ for the primary, it may actually be an upper limit.

From Kepler's third law the semimajor axis was computed and then with Equation (2) of Eggleton (1983) we estimated a Roche-lobe radius of 184 $R_\odot$ for the M giant. The radius of 86 $R_\odot$ (Schmutz et al. 1994) would fill just 47% of that Roche lobe. However, the infrared photometry of Rutkowski et al. (2007) shows that SY Mus has ellipsoidal variations. According to Shahbaz (1998) and Orosz & Houschildt (2000), if a component of a binary system substantially fills its Roche lobe, models predict that its absorption lines will have distorted profiles and its $v \sin i$ value will change with phase. Thus, for symbiotic stars Quiroga et al. (2002) concluded that caution is in order if $v \sin i$ values are used to estimate the radii of the cool giants. They argued that estimates from ellipsoidal light variations provide a much better way of determining the radii of the cool giants in symbiotic systems.

For SY Mus we looked for the predicted line profile distortions, but to the limit of our resolution and signal-to-noise ratios, the profiles are symmetric. In addition, Gałan et al. (2016) used just a single value of $v \sin i$, which provided a good fit to the various spectra that they analyzed for abundances.

From a preliminary analysis of their SY Mus *JHK* light curves Rutkowski et al. (2007) determined a much larger cool giant radius of 135 $R_\odot$, and found a Roche lobe filling factor of 0.83. Their radius for the cool giant is about 60% larger than the value from its $v \sin i$. To produce the larger radius would require a rotational velocity of 11 km s^{-1}.

We believe that the preliminary light curve modeling results should also be viewed with caution. As noted by Rutkowski et al. (2007) the light curves of symbiotics, even in the infrared may have significant complications, due to, for example, outbursts or hot companion accretion disks. In the case of SY Mus the best fits shown by Rutkowski et al. (2007) for the ellipsoidal variations of SY Mus only approximately fit the light curves, and those authors provided no errors for any of their model parameters. Thus, of the three different radius determinations mentioned above, we prefer to adopt the one from the spectroscopic gravity. The uncertainty of that value, 114 $\pm$ 27 $R_\odot$, overlaps the 135 $R_\odot$ value from the ellipsoidal solution.

While SY Mus is 65° from the Galactic center in longitude, it is only 4° below the Galactic plane. With $E_{B-V} = 0.45$ from Pereira et al. (1995) and the extinction relation of Schlegel et al. (1998), we find the extinction in the K band to be $A_K = 0.17$. From the M_K value determined above this results in a distance of 1.5 $\pm$ 0.3 kpc. Our value is substantially larger than that of Schmutz et al. (1994) primarily because of the much larger radius that we have adopted. Our various derived quantities are summarized in Table 7.

Table 7
Assumed and Derived Properties of SY Mus

Parameter	Value	Reference
Cool giant:		
M ($M_\odot$)	1.5 (Adopted)	This work
$v \sin i$ (km s^{-1})	7 $\pm$ 1	Schmutz et al. (1994)
R ($R_\odot$)	114 $\pm$ 27	This work
$T_{\rm eff}$ (K)	3400 $\pm$ 100	Gałan et al. (2016)
L ($L_\odot$)	1556 $\pm$ 760	This work
$M_{\rm bol}$ (mag)	−3.25 $\pm$ 0.52	This work
M_K (mag)	−6.37 $\pm$ 0.52	This work
Hot component:		
M ($M_\odot$)	0.50	This work
System:		
i (degree)	84	This work
Distance (kpc)	1.5 $\pm$ 0.3	This work

7. HEN 3-828 = SS 73-37 = WRAY 15-1022

7.1. Short History

Sanduleak & Stephenson (1973) carried out an objective prism survey of the southern Milky Way, looking for stars with strong emission lines. In their 1973 list they characterized object number 37 as a Z Andromedae like star with a possible O III 5007 Å emission feature, and so they were the first to identify it as a likely symbiotic star. Several years later, Henize (1976) listed it as number 828 in his objective prism survey search for southern emission line stars. He found it to have a trace of continuum intensity and a strong Hα emission line. Allen (1978) obtained low dispersion slit spectra of 89 emission line stars identified by Sanduleak & Stephenson (1973). For Hen 3-828 Allen (1978) found weak TiO bands, weak Fe II, He II, and [O III] emission as well as relatively strong He I and [Fe VII] emission. As a result, he concluded that it is indeed a symbiotic star. From a 2 μm spectrum taken with the Anglo-Australian Telescope Allen (1980) determined a spectral class of M6. Allen (1984) listed it in his catalog of symbiotic stars and presented a low-dispersion spectrum that covered the wavelength range 3400–7500 Å and displayed numerous emission features in that spectral region. Spectra obtained in 1987 and 1991 show that Hen 3-828 had a greatly enhanced continuum in 1991 that resulted in many of the emission lines seen in 1987 becoming undetectable (Gutierrez-Moreno et al. 1999). Along with over 90 other symbiotics Mürset & Schmid (1999) classified the spectrum of Hen 3-828 based on near-infrared spectra. They assigned it a spectral class of M6, identical to that of Allen (1980). Recently, Gałan et al. (2016) found the M giant of Hen 3-828 to have a solar iron abundance, [Fe/H] = −0.03 $\pm$ 0.11.

7.2. Spectroscopic Orbit

Between 2001 March and 2010 March we acquired 18 spectra of Hen 3-828 from which we determined radial velocities (Table 8). An analysis of these velocities resulted in a preliminary period of 660.0 days. A solution with all elements allowed to vary resulted in an orbit with a period of 659.0 $\pm$ 3.6 days and an eccentricity of 0.12 $\pm$ 0.07. Comparing circular and eccentric orbital-element solutions, the

Table 8
Radial Velocities of Hen 3-828

HJD −2400000	Phase	Velocity (km s^{-1})	$O-C$ (km s^{-1})	Observatory[a]
51992.022	0.131	−9.4	0.1	MSO
51995.056	0.136	−10.4	−0.7	MSO
52046.995	0.214	−14.8	−1.7	MSO
52094.971	0.287	−18.0	−1.3	MSO
52134.951	0.348	−20.2	−0.8	MSO
52349.238	0.672	−18.9	−0.3	MSO
52356.064	0.682	−18.2	−0.1	MSO
52398.964	0.747	−16.1	−1.1	MSO
52446.898	0.820	−11.6	−0.1	MSO
52506.947	0.911	−7.5	0.7	MSO
52686.807	0.183	−9.7	1.9	Gem S
52749.605	0.278	−15.3	1.0	Gem S
52849.516	0.429	−19.9	2.1	Gem S
52986.848	0.637	−20.6	−0.6	Gem S
53098.630	0.807	−13.3	−1.2	Gem S
53714.848	0.740	−14.3	1.1	Gem S
53828.608	0.912	−6.6	1.5	Gem S
55285.700	0.118	−9.7	−0.7	Gem S

Note.
[a] MSO—Mount Stromlo Observatory, Gem S—Gemini South Observatory.

precepts of Lucy & Sweeney (1971) indicate that the circular orbit, which has a period of 660.5 days, is to be preferred, and thus, those orbital elements are given in Table 9. A phase plot of the radial velocities compared to the computed velocity curve is shown in Figure 5. As with the phase plot of SY Mus, zero phase is a time of maximum radial velocity.

7.3. Pulsation Period Search

A search of the 18 residual velocities produced several possible periods between 10 and 25 days. However, as noted earlier, pulsation periods for M giants typically range from 30 to 200 days (Lebzelter & Hinkle 2002). An examination of the phase plots for the best periods does not produce convincing evidence that they are real.

7.4. Discussion

With a period of 660.5 days the circular orbit of Hen 3-828 is typical of symbiotic systems analyzed to date, which peak around 600 days and generally have circular orbits at such periods (Mikołajewska 2012).

Using the mass function, we find that for a range of M giant masses from 2.5 to 1.0 $M_\odot$, the minimum secondary mass ($\sin i = 1$) goes from 0.70 to 0.41. Unfortunately, Hen 3-828 was not one of the extensive number of symbiotic systems that had its light curve analyzed by Gromadzki et al. (2013). Thus, there is no indication as to whether or not it eclipses. Thus, if we adopt a typical mass of 1.5 $M_\odot$ for the M giant and an inclination of 60°, the mass function value of 0.034 $M_\odot$ results in a mass of 0.60 $M_\odot$ for the compact secondary. For this mass combination, the secondary to primary mass ratio is 0.4.

From the relation between the initial and final mass for DA white dwarfs (Kalirai et al. 2008) a 0.60 $M_\odot$ white dwarf evolved from a 1.9 $M_\odot$ main sequence star. This is more massive than the adopted primary mass of 1.5 $M_\odot$. The cool giant has near solar abundances (Gałan et al. 2016), so the evolutionary age of 3×10^9 years (Girardi et al. 2000) also is consistent with the data.

Table 9
Orbital Elements and Related Parameters of Hen 3-828

Parameter	Value
P (days)	660.5 ± 4.5
T (HJD)	2453226.4 ± 6.1
γ (km s^{-1})	−14.87 ± 0.31
K (km s^{-1})	7.92 ± 0.55
e	0.0 (adopted)
$a \sin i$ (10^6 km)	71.9 ± 5.0
$f(m)$ ($M_\odot$)	0.0340 ± 0.0071
Standard error of an observation of unit weight (km s^{-1})	1.3

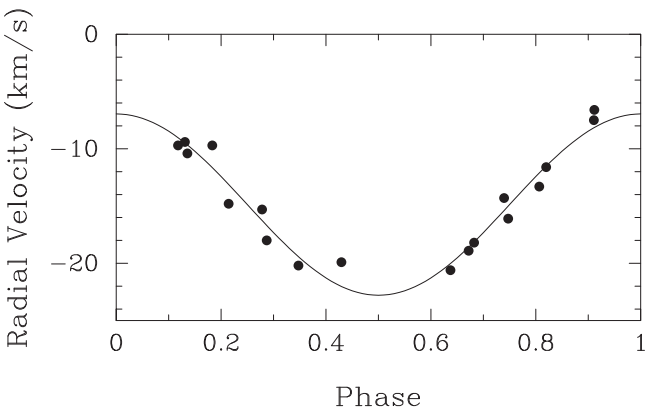

Figure 5. The M giant radial velocities of Hen 3-828 (filled circles) are compared with its computed circular orbit (solid line). Zero phase is a time of maximum velocity.

Following Schmutz et al. (1994) and Mürset et al. (2000), we assume that the M giant of Hen 3-828 is synchronously rotating. With that assumption and the orbital period of 660.5 days, its projected rotational velocity can be used to estimate its minimum radius. For Hen 3-828 Gałan et al. (2016) has determined a $v \sin i$ value of 7.9 ± 0.5 km s^{-1}, This value produces a minimum radius (i.e., $\sin i = 1$) of 103 ± 7 $R_\odot$. With the adopted inclination of 60° and the assumption that the orbital and rotational axes are parallel, the radius of the M giant is increased from 103 to 119 ± 8 $R_\odot$.

Adopting masses of 1.5 and 0.6 $M_\odot$ for the M giant and its companion, respectively, we used Kepler's third law to determine the semimajor axis of the orbit. Then with Equation (2) of Eggleton (1983), we estimated an M giant Roche-lobe radius of 188 $R_\odot$. Our estimated radius of 119 $R_\odot$ would fill 63% of that Roche lobe. Such a moderate filling factor would likely not produce detectable ellipsoidal variability.

For the cool giant we adopt an effective temperature of 3300 ± 100 K (Gałan et al. 2016), which is consistent with its spectral class of M6 (Mürset & Schmid 1999). That temperature plus our estimated radius, 119 ± 8 $R_\odot$, results in a luminosity of 1505 ± 272 $L_\odot$, which corresponds to $M_{\rm bol} = -3.21 \pm 0.20$ mag.

Like the previous two symbiotics, Munari et al. (1992) included Hen 3-828 in their photometric survey of symbiotic stars. Their values for V, K, and $J-K$ are 14.30, 7.17, and 1.48 mag, respectively. To estimate the distance to Hen 3-828, we adopted those values of its K mag and $J-K$ color. We then used the analytic expression of Bessell & Wood (1984) to

Table 10
Assumed and Derived Properties of Hen 3-828

Parameter	Value	Reference
Cool giant:		
M ($M_\odot$)	1.5 (Adopted)	This work
$v \sin i$ (km s^{-1})	7.9 ± 0.5	Gałan et al. (2016)
R ($R_\odot$)	119 ± 8	This work
$T_{\rm eff}$ (K)	3300 ± 100	Gałan et al. (2016)
L ($L_\odot$)	1505 ± 272	This work
$M_{\rm bol}$ (mag)	−3.21 ± 0.20	This work
M_K (mag)	−6.38 ± 0.20	This work
Hot component:		
M ($M_\odot$)	0.60	This work
System:		
i (degree)	60 (Adopted)	This work
Distance (kpc)	4.3 ± 0.4	This work

obtain a bolometric correction at K. This, combined with our value of $M_{\rm bol}$ from the M giant's radius, produces $M_K = -6.38 \pm 0.20$ mag. Hen 3-828 lies about 57° from the Galactic center but only 5° above the Galactic plane. Gutierrez-Moreno et al. (1999) determined an extinction value in the K band of $A_K = 0.4$. Adopting this value results in a distance of 4.3 ± 0.4 kpc, which is significantly larger than the value of 1.6 kpc estimated by Gutierrez-Moreno et al. (1999). The various derived quantities are summarized in Table 10.

8. AR PAV = HIP 89886 = HEN 3-1649 = HV 7860

8.1. Short History

Mayall (1937) discovered an eclipsing binary with unusual characteristics that was given the identification Harvard Variable or HV 7860. It had a long eclipse period of 605 days, and its spectrum was found to have Balmer emission with those lines showing absorption on the blue side of the lines. On one plate He II at 4686 Å was also in emission. Thus, Mayall classified it initially as a P Cygni type star. However, from photographic plates covering 47 years, she found that the maximum magnitude of the star differed by nearly 3 mag with no apparent regularity, a result extremely unusual for a P Cygni type star. A few years later Merrill & Burwell (1943) listed AR Pav in their extensive catalog of Ae and Be stars, but eventually its true nature came to light. In 1954 Thackeray (1954) reported on spectra that he obtained of AR Pav at blue and yellow wavelengths. He noted that the spectroscopic characteristics of the star placed it with a group of about 20 known symbiotic objects that had features of both high temperature nebular lines and low temperature TiO absorption. Significant strides in the understanding of the system occurred two decades later when Thackeray & Hutchings (1974) proposed that the system was a binary with an M giant filling its Roche lobe and losing mass to the second star.

Allen (1984) included AR Pav in his symbiotic star catalog and provided a low-resolution spectrum of the 3600–7100 Å region that showed a number of emission features and its M giant continuum. From a 2 μm spectrum Allen (1980) assigned AR Pav an M6 spectral class, while Mürset & Schmid (1999) determined a slightly earlier class of M5.

Schild et al. (2001) obtained the first orbital solution for the cool giant, estimated its basic properties, and examined the earlier results of Thackeray & Hutchings (1974), who measured lines linked to the hot companion. Shortly thereafter, Quiroga et al. (2002) determined an independent orbital solution from velocities of the M giant and also determined orbits for the velocities of various proxy lines associated with the hot component. Rutkowski et al. (2007) carried out a preliminary analysis of its near-infrared light curves, which show ellipsoidal light variability.

8.2. Spectroscopic Orbit

From 2001 March through 2010 June we obtained 16 spectra of AR Pav (Table 11) and determined radial velocities of the M giant. With our velocities we first computed an orbit with all elements allowed to vary. That solution resulted in an orbital period of 604.3 ± 1.3 days and an eccentricity of 0.042 ± 0.034. According to the precepts of Lucy & Sweeney (1971), the small eccentricity and its relatively large uncertainty indicate that a circular orbit is to be preferred. So following Schild et al. (2001) and Quiroga et al. (2002), we obtained a circular-orbit solution of our velocities that assumed the 604.5 day photometric period of Bruch et al. (1994). To obtain a solution with all the absorption line radial velocities, we examined the orbital solutions of Schild et al. (2001) and Quiroga et al. (2002) as well as that of our circular orbit. From a comparison of the systemic velocities and the variances of the three solutions, for the velocities of Schild et al. (2001) we added 1.6 km s^{-1} and assigned a weight of 0.3 to each of them. Similarly, for the velocities of Quiroga et al. (2002) we added 1.5 km s^{-1} and assigned a weight of 0.1 to each of them. Our velocities were given unit weights. The three sets of velocities span 19.6 years, and so we allowed the period to be a free parameter. The resulting spectroscopic period is 603.93 ± 0.63 days. This period is within 1σ of the photometric period of 604.5 days. Skopal et al. (2000) determined the same 604.5 day average photometric period as Bruch et al. (1994) but concluded that the orbital period was decreasing with time. Skopal et al. (2001) noted that the most recent minima available, 1998 December and 2000 August, which are in the middle of the time span of our spectroscopic observations, produced a period of 603.9 ± 0.5 days. The 51 radial velocities from the three sources are listed in Table 11, and the elements from our joint data solution are given in Table 12. For comparison, the separate solutions of Schild et al. (2001), Quiroga et al. (2002), and our independent circular-orbit solution are also give in the latter table. A phase plot of the radial velocities compared to the computed velocity curve is shown in Figure 6. Zero phase is a time of maximum velocity.

8.3. Pulsation Period Search

Because of the low rms value of our velocities to the combined orbital fit, we did not examine their velocity residuals for possible pulsation periods. However, the velocities of Schild et al. (2001) and Quiroga et al. (2002) have much larger velocity residuals to the combined fit. A period of 130.8 days was found when the two sets of residuals were combined, but after separating the two data sets, it was only found in the 13 residual velocities of Quiroga et al. (2002), and so we do not believe that this period is real.

Table 11
Radial Velocities of AR Pav

HJD −2400000	Phase	Velocity (km s^{-1})	$O-C$ (km s^{-1})	Weight	Observatory[a]
48201.500	0.853	−57.5	3.1	0.1	CASLEO
48511.600	0.366	−73.9	−0.2	0.3	LSO
48553.800	0.436	−75.8	0.5	0.3	LSO
48757.700	0.774	−66.7	−1.4	0.3	LSO
48852.700	0.931	−53.5	4.0	0.1	CASLEO
49131.900	0.393	−76.3	−1.4	0.3	LSO
49289.500	0.654	−73.1	−0.4	0.3	LSO
49291.500	0.657	−72.0	0.5	0.3	LSO
49292.500	0.659	−73.4	−1.0	0.3	LSO
49550.600	0.087	−59.8	−1.8	0.3	LSO
49576.600	0.130	−59.0	0.7	0.3	LSO
49577.700	0.131	−61.1	−1.3	0.3	LSO
49657.600	0.264	−68.8	−1.1	0.3	LSO
49861.800	0.602	−75.8	−0.7	0.3	LSO
49866.800	0.610	−73.1	1.7	0.3	LSO
49941.700	0.734	−74.5	−6.6	0.1	CASLEO
50037.500	0.893	−60.2	−1.4	0.3	LSO
50038.500	0.894	−59.1	−0.4	0.3	LSO
50173.900	0.119	−56.6	2.6	0.3	LSO
50266.700	0.272	−68.4	−0.1	0.3	LSO
50286.600	0.305	−70.0	0.4	0.3	LSO
50302.700	0.332	−69.4	2.5	0.3	LSO
50302.800	0.332	−72.0	−0.1	0.3	LSO
50303.700	0.334	−72.0	0.0	0.3	LSO
50649.800	0.907	−56.2	2.0	0.3	LSO
50879.900	0.288	−71.5	−2.2	0.1	CASLEO
50880.900	0.289	−70.5	−1.1	0.1	CASLEO
51064.600	0.593	−71.5	3.9	0.1	CASLEO
51238.900	0.882	−60.5	−1.3	0.1	CASLEO
51324.800	0.024	−54.5	2.1	0.1	CASLEO
51422.600	0.186	−63.5	−0.7	0.1	CASLEO
51628.900	0.528	−78.5	−1.5	0.1	CASLEO
51630.900	0.531	−77.5	−.5	0.1	CASLEO
51754.700	0.736	−68.5	−0.8	0.1	CASLEO
51756.700	0.739	−66.5	1.0	0.1	CASLEO
51995.331	0.135	−59.7	0.3	1.0	MSO
52047.306	0.221	−65.9	−1.0	1.0	MSO
52093.265	0.297	−70.9	−1.1	1.0	MSO
52131.208	0.360	−72.4	1.0	1.0	MSO
52200.019	0.473	−77.4	−0.4	1.0	MSO
52354.313	0.729	−67.8	0.4	1.0	MSO
52400.298	0.805	−64.0	−0.7	1.0	MSO
52403.139	0.810	−63.7	−0.7	1.0	MSO
52451.122	0.889	−58.5	0.4	1.0	MSO
52503.057	0.975	−56.2	0.4	1.0	MSO
52574.906	0.094	−58.5	−0.2	1.0	MSO
54973.904	0.067	−58.1	−0.7	1.0	CTIO
54988.936	0.091	−56.9	1.3	1.0	Gem S
55037.801	0.172	−61.8	0.2	1.0	CTIO
55342.789	0.677	−70.3	1.1	1.0	Gem S
55364.898	0.714	−69.6	−0.4	1.0	CTIO

Note.
[a] CASLEO—Complejo Astronómico el Leoncito, LSO—La Silla Observatory, MSO—Mount Stromlo Observatory, Gem S—Gemini South Observatory, CTIO—Cerro Tololo Inter-American Observatory.

8.4. Discussion

Although AR Pav was included in the photometric survey of symbiotic stars by Munari et al. (1992), they only determined its $UBVR_cI_c$ magnitudes. However, Glass & Webster (1973) obtained infrared measures in the *JHKL* bands for a number of emission line objects including AR Pav. The values for V, K, and $J-K$ are 11.14, 7.10, and 1.14 mag, respectively.

Mikołajewska (2012) examined the general orbital characteristics of S-type symbiotics and found that most have periods around 600 days and circular orbits. With a period of 603.9 days and a circular orbit, AR Pav, like SY Mus and Hen 3-828, is another typical system.

Schild et al. (2001) estimated a mass of 2.0 $M_\odot$ for the M giant from a comparison of its properties with evolutionary tracks. Quiroga et al. (2002) determined an even higher mass of 2.5 $M_\odot$ from their double-lined orbit and an orbital inclination of ∼90°. To determine the velocity curve of the secondary, which enabled them to compute the $m \sin^3 i$ values for both stars, they measured velocities of the broad emission wings of H I and He II, which they stated form in the region near the hot companion and, thus, they believed could be used as proxy lines for that star. Their masses of 2.5 for the cool giant primary and 1.0 for the hot compact secondary are both at the high end of masses estimated for the components of symbiotic binaries (Mikołajewska 2003). For AR Pav the large masses of Quiroga et al. (2002) depend heavily on the veracity of the semi-amplitude of the hot component. Another property of the orbit, however, suggests that the M giant mass is significantly smaller than 2.5 $M_\odot$. The center-of-mass velocity of AR Pav is quite large, −66.8 km s^{-1}, offering evidence that the system is a member of the old disk population. Old disk stars have masses in the range of 1.0–1.5 $M_\odot$ (Wallerstein 1981). Thus, we adopt a mass of 1.5 $M_\odot$ for the M giant.

The fact that AR Pav is an eclipsing binary restricts its orbital inclination. However, Quiroga et al. (2002) have pointed out that the eclipses of AR Pav are not total because the $B-V$ color at mid-eclipse of the hot component is that of an early-G star rather than an M giant. Schild et al. (2001) have argued that the inclination is greater than 79°, while Quiroga et al. (2002) have set a lower limit of 70°. When Rutkowski et al. (2007) analyzed the ellipsoidal variations seen in the infrared light curves of AR Pav, their model resulted in a value of 74° for the orbital inclination. Given the above results, we have assumed a value of 75°.

So with an adopted M giant mass of 1.5 $M_\odot$ and orbital inclination of 75°, the mass function value of 0.069 from our M giant orbit results in a mass of 0.72 $M_\odot$ for the hot compact component. For this mass combination, the secondary to primary mass ratio is 0.48. From the initial mass–final mass relation for white dwarfs (Kalirai et al. 2008) the initial mass of the current white dwarf was 3 $M_\odot$. While our hot component mass is smaller than that estimated by Schild et al. (2001) and Quiroga et al. (2002), it is still larger than the typical mass of 0.5 $M_\odot$ found for other hot components of S-type symbiotics (Mikołajewska 2003). Reducing the cool giant mass to 1.2 $M_\odot$ produces a mass of 0.63 $M_\odot$ for the hot compact companion and an initial mass of 2.2 $M_\odot$.

With our masses for the M giant and its companion, we used Kepler's third law to determine the semimajor axis of the orbit. Then with Equation (2) of Eggleton (1983), we estimated a Roche-lobe radius of 174 $R_\odot$ for the M giant. The radius of 130 $R_\odot$ for AR Pav, determined by Schild et al. (2001) from their $v \sin i$ of 11 ± 2 km s^{-1} and the assumption of synchronous rotation, would fill 75% of that Roche lobe. However, Quiroga et al. (2002) cautioned that the tidal distortion of the giant may bias the $v \sin i$ measurement. From their ellipsoidal variability analyses Rutkowski et al. (2007) found a much

Table 12
Orbital Elements and Related Parameters of AR Pav

Parameter	Schild et al. (2001)	Quiroga et al. (2002)	Our Solution	Combined Solution
P (days)	604.5 (adopted)	604.5 (adopted)	604.5 (adopted)	603.93 ± 0.63
T_0 (HJD)	2448139.0[a] ± 4.0	...	2453725.7 ± 2.4	2452518.0 ± 2.0
γ (km s^{-1})	−68.4 ± 0.3	−68.3 ± 0.8	−66.83 ± 0.21	−66.84 ± 0.17
K (km s^{-1})	9.6 ± 0.4	11.4 ± 1.2	10.36 ± 0.34	10.33 ± 0.27
e	0.0 (adopted)	0.0 (adopted)	0.0 (adopted)	0.0 (adopted)
$a \sin i$ (10^6 km)	...	...	86.1 ± 2.8	85.8 ± 2.2
$f(m)$ ($M_\odot$)	0.055 ± 0.007	...	0.0696 ± 0.0068	0.0691 ± 0.0053
Standard error of an observation of unit weight (km s^{-1})	...	...	0.8	0.8

Note.
[a] Time of hot component eclipse.

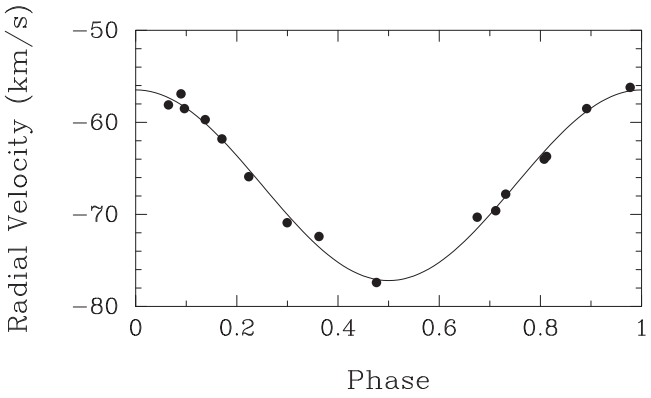

Figure 6. The M giant radial velocities of AR Pav compared with its computed circular orbit (solid line). Filled circles—our velocities, open circles—ESO, and open triangles—CASLEO. Zero phase is a time of maximum velocity.

larger radius of the giant, 190 $R_\odot$, which if the star is synchronously rotating, would result in a very rapid rotational velocity of 16 km s^{-1}, nearly 50% larger than that measured by Schild et al. (2001). Rutkowski et al. (2007) also determined a much higher Roche lobe filling factor of 96% from their infrared analyses.

The preliminary ellipsoidal model fits for AR Pav should be viewed with even more caution than those of SY Mus. AR Pav is an active symbiotic that has extensive optical variability (Skopal et al. 2000). Even in their infrared light curves Rutkowski et al. (2007) found an additional source of light, which they characterized as either a thick accretion disk or an extended envelope surrounding the compact companion. As a result, Rutkowski et al. (2007) had some significant difficulty in modeling the ellipsoidal light curve of AR Pav. The solution that they presented is not a particularly good fit to the data, and they gave no uncertainties for their model parameters. Thus, we have chosen to adopt the smaller radius value determined by Schild et al. (2001).

From the M5 spectral class (Mürset & Schmid 1999) of the giant we assume an effective temperature of 3400 ± 100 K, a value adopted for other M5 stars by Gałan et al. (2016). That value and the estimated radius of 130 ± 25 $R_\odot$ (Schild et al. 2001), result in a luminosity of 2023 ± 793 $L_\odot$, which converts to $M_{\rm bol} = -3.54 \pm 0.45$ mag. Because we have used the radius determined by Schild et al. (2001) it is not surprising that our luminosity is quite similar to theirs.

AR Pav was observed by the *Hipparcos* satellite, and the new parallax reduction by van Leeuwen (2007) resulted in a value of 1.32 ± 2.34 mas. This produces a distance of 760 pc, but of course the uncertainty is much larger than the actual value, making the result of little significance. Thus, to estimate the distance to AR Pav, we adopted its K mag and $J-K$ color from Glass & Webster (1973). We then used the analytic expression of Bessell & Wood (1984), involving that color, to obtain a bolometric correction at K. This, combined with our value of $M_{\rm bol}$ from the M giant's radius, produces $M_K = -6.40 \pm 0.45$ mag. Its position in the sky is close to the Galactic center in longitude, being just 31.°5 away, but it is nearly 22° below the Galactic plane, so extinction is not likely to be extensive. With $E_{B-V} = 0.3$ (Slovak 1982; Kenyon & Webbink 1984) and the extinction relation of Schlegel et al. (1998), we find the extinction in the K band to be $A_K = 0.11$. This results in a distance of 4.8 ± 1.0 kpc. Our distance for AR Pav is similar to that found by others (see e.g., Kenyon & Webbink 1984; Schild et al. 2001) and places it well outside the Galactic plane. The various derived quantities are summarized in Table 13.

Table 13
Assumed and Derived Properties of AR Pav

Parameter	Value	Reference
Cool giant:		
M ($M_\odot$)	1.5 (Adopted)	This work
$v \sin i$ (km s^{-1})	11 ± 2	Schild et al. (2001)
R ($R_\odot$)	130 ± 25	Schild et al. (2001)
$T_{\rm eff}$ (K)	3400 ± 100	Gałan et al. (2016)
L ($L_\odot$)	2023 ± 793	This work
$M_{\rm bol}$ (mag)	−3.54 ± 0.45	This work
M_K (mag)	−6.40 ± 0.45	This work
Hot component:		
M ($M_\odot$)	0.72	This work
System:		
i (degree)	75 (Adopted)	This work
Distance (kpc)	4.8 ± 1.0	This work

We thank NOAO for enabling several aspects of this research, including access to time on the Gemini and SMARTS telescopes, and travel support for K. Hinkle and R. Joyce. This paper is based in part on observations obtained at the Gemini Observatory, which is operated by the Association of Universities for Research in Astronomy, Inc., under a

cooperative agreement with the NSF on behalf of the Gemini partnership: the National Science Foundation (United States), the Particle Physics and Astronomy Research Council (United Kingdom), the National Research Council (Canada), CONICYT (Chile), the Australian Research Council (Australia), CNPq (Brazil), and CONICRT (Argentina). The observations were acquired with the Phoenix infrared spectrograph, which was developed and is operated by the National Optical Astronomy Observatory. The Gemini/Phoenix spectra were obtained as part of programs GS-2003A-DD-1, GS-2003B-DD-1, GS-2004A-DD-1, and GS-2006A-DD-1. Observations were also obtained at the Gemini South Observatory as part of Poor Weather Queue program number GS-2010A-Q-79. Several additional observations were acquired through the NOAO share of time on one of the SMARTS consortium telescopes. Astronomy at Tennessee State University is supported by the state of Tennessee through its Centers of Excellence program. We have made use of the SIMBAD database, operated by CDS in Strasbourg, France, as well as NASA's Astrophysics Data System Abstract Service. Finally, we thank the referee for useful comments that improved our work.

REFERENCES

Allen, D. A. 1978, MNRAS, 184, 601
Allen, D. A. 1980, MNRAS, 192, 521
Allen, D. A. 1984, PASAu, 5, 369
Batten, A. H., Fletcher, J. M., & MacCarthy, D. G. 1989, PDAO, 17, 1
Belczyński, K., Mikołajewska, J., Munari, U., Ivison, R. J., & Friedjung, M. 2000, A&AS, 146, 407
Bessell, M. S., & Wood, P. R. 1984, PASP, 96, 247
Bruch, A, Niehues, M, & Jones, A. F. 1994, A&A, 287, 829
Cannon, A. J., & Pickering, E. C. 1914, Harvard Circ., 184, 1
Dumm, T., & Schild, H. 1998, NewA, 3, 137
Dumm, T., Schmutz, W., Schild, H., & Nussbaumer, H. 1999, A&A, 349, 169
Dyck, H. M., van Belle, G. T., & Thompson, R. R. 1998, ApJ, 116, 981
Eggleton, P. P. 1983, ApJ, 269, 368
Fekel, F. C., Hinkle, K. H., Joyce, R. R., & Wood, P. R. 2010, AJ, 139, 1315
Fekel, F. C., Hinkle, K. H., Joyce, R. R., & Wood, P. R. 2015, AJ, 150, 48
Fekel, F. C., Hinkle, K. H., Joyce, R. R., Wood, P. R., & Howarth, I. D. 2008, AJ, 136, 146
Fekel, F. C., Joyce, R. R., Hinkle, K. H., & Skrutskie, M. F. 2000, AJ, 119, 1375
Fitzpatrick, M. J. 1993, in ASP Conf. Ser. 52, Astronomical Data Analysis Software and Systems II, ed. R. J. Hanish, R. V. J. Brissenden, & J. Barnes (San Francisco, CA: ASP), 472
Gałan, C., Mikołajewska, J., Hinkle, K. H., & Joyce, R. R. 2016, MNRAS, 455, 1282
Girardi, L., Bressan, A., Bertelli, G., & Chiosi, C. 2000, A&AS, 141, 371
Glass, I. S., & Webster, B. L. 1973, MNRAS, 165, 77
Greenstein, N. K. 1937, BHarO, 906, 3
Gromadzki, M., Mikołajewska, J., & Soszynski, I. 2013, AcA, 63, 405
Gutierrez-Moreno, A., Moreno, H., & Costa, E. 1999, PASP, 111, 571
Harries, T. J., & Howarth, I. D. 2000, A&A, 361, 139
Hartig, E., Cash, J., Hinkle, K. H., et al. 2014, AJ, 148, 123
Henize, K. G. 1952, ApJ, 115, 133
Henize, K. G. 1976, ApJS, 30, 491
Hinkle, K. H., Cuberly, R. W., Gaughan, N. A., et al. 1998, Proc. SPIE, 3354, 810
Hinkle, K. H., Fekel, F. C., & Joyce, R. R. 2009, AJ, 692, 1360
Hinkle, K. H., Fekel, F. C., Joyce, R. R., & Wood, P. R. 2013, ApJ, 770, 28
Hinkle, K. H., Fekel, F. C., Joyce, R. R., et al. 2006, ApJ, 641, 479
Hut, P. , 1981, A&A, 99, 126
Istrate, A. G., Marchant, P., Tauris, T. M., et al. 2016, A&A, 595, A35
Jorissen, A., Van Eck, S., Dermine, T., Van Winckel, H., & Gorlova, N. 2012, BaltA, 21, 39
Joyce, R. R. 1992, in ASP Conf. Ser. 23, Astronomical CCD Observing and Reduction Techniques, ed. S. Howell (San Francisco, CA: ASP), 258
Joyce, R. R., Hinkle, K. H., Meyer, M. R., & Skrutskie, M. F. 1998, Proc. SPIE, 3354, 741
Kalirai, J. S., Hansen, B. M. S., Kelson, D. D., et al. 2008, ApJ, 676, 594
Keenan, P. C., & McNeil, R. C. 1989, ApJS, 71, 245
Kenyon, S. J., & Bateson, F. M. 1984, PASP, 96, 321
Kenyon, S. J., Michalitsianos, A. G., Lutz, J. H., & Kafatos, M. 1985, PASP, 97, 268
Kenyon, S. J., & Webbink, R. F. 1984, ApJ, 279, 252
Kučinskas, A., Hauschildt, P. H., Ludwig, H.-G., et al. 2005, A&A, 442, 281
Lebzelter, T., & Hinkle, K. H. 2002, A&A, 393, 563
Lucy, L. B., & Sweeney, M. A. 1971, AJ, 76, 544
Luna, G. J. M., Sokoloski, J. L., Mukai, K., & Nelson, T. 2013, A&A, 559A, 6
Mayall, M. W. 1937, AnHar, 105, 491
Merrill, P. W., & Burwell, C. G. 1943, ApJ, 98, 153
Michalitsianos, A. G., Kafatos, M., Feibelman, W. A., & Wallerstein, G. 1982, A&A, 109, 136
Mikołajewska, J. 2001, in IAU Coll. 183, Small Telescope Astronomy on Global Scales, ed. W.-P. Chen, C. Lemme, & B. Paczyński (San Francisco, CA: ASP), 167
Mikołajewska, J. 2003, in ASP Conf. Ser. 303, Symbiotic Stars Probing Stellar Evolution, ed. R. L. M. Corradi, J. Mikołajewska, & T. J. Mahoney (San Francisco, CA: ASP), 9
Mikołajewska, J. 2011, in IAU Symp. 281, Symbiotic Stars as Possible Progenitors of SNe Ia: Binary Parameters and Overall Outlook, ed. R. Di Stefano, M. Orio, & M. Moe (Cambridge: Cambridge Univ. Press), 162
Mikołajewska, J. 2012, BaltA, 21, 5
Miszalski, B., & Mikołajewska, J. 2014, MNRAS, 440, 1410
Miszalski, B., Mikołajewska, J., & Udalski, A. 2013, MNRAS, 432, 3186
Motz, L., & Duveen, A. 1977, Essentials of Astronomy (New York: Columbia Univ. Press)
Munari, U., Yudin, B. F., Taranova, O. G., et al. 1992, A&AS, 93, 383
Mürset, U., Dumm, T., Isenegger, S., et al. 2000, A&A, 353, 952
Mürset, U., & Schmid, H. M. 1999, A&AS, 137, 473
Orosz, J. A., & Houschildt, P. H. 2000, A&A, 364, 265
Percy, J. R., Wilson, J. B., & Henry, G. W. 2001, PASP, 113, 983
Pereira, C. B., Landaberry, S. J. C., & da Conceicao, F. 1998, AJ, 116, 1971
Pereira, C. B., Vogel, M., & Nussbaumer, H. 1995, A&A, 293, 783
Pojmanski, G. 2002, AcA, 52, 397
Quiroga, C., Mikołajewska, J., Brandi, E., Ferrer, O., & Garcia, L. 2002, A&A, 387, 139
Rutkowski, A., Mikołajewska, J., & Whitelock, P. A. 2007, BaltA, 16, 49
Sanduleak, N., & Stephenson, C. B. 1973, ApJ, 185, 899
Scarfe, C. D., Batten, A. H., & Fletcher, J. M. 1990, PDAO, 18, 21
Schild, H., Dumm, T., Mürset, U., et al. 2001, A&A, 366, 972
Schlegel, D. J., Finkbeiner, D. P., & Davis, M. 1998, ApJ, 500, 525
Schmid, H. M., & Schild, H. 2002, A&A, 395, 117
Schmutz, W., Schild, H., Mürset, U., & Schmid, H. M. 1994, A&A, 288, 819
Shahbaz, T. 1998, MNRAS, 298, 153
Skopal, A., Djurasevic, G., Jones, A., et al. 2000, MNRAS, 311, 225
Skopal, A., Kohoutek, L., Jones, A., & Drechsel, H. 2001, IBVS, 5195, 1
Slovak, M. H. 1982, PhD thesis, Univ. Texas
Soszyński, I., Wood, P. R., & Udalski, A. 2013, ApJ, 779, 167
Thackeray, A. D. 1954, Obs, 74, 257
Thackeray, A. D., & Hutchings, J. B. 1974, MNRAS, 167, 319
Uitterdijk, J. 1934, BAN, 7, 177
van Leeuwen, F. 2007, Hipparcos, The New Reduction of the Raw Data (Dordrecht: Springer)
Wallerstein, G. 1981, Obs, 101, 172
Webster, B. L., & Allen, D. A. 1975, MNRAS, 171, 171
Whitelock, P. A. 1987, PASP, 99, 573
Zahn, J.-P. 1977, A&A, 57, 383